JOURNAL OF BACTERIOLOGY, Aug. 2007, p. 5463–5471 Vol. 189, No. 15
0021-9193/07/$08.00+0 doi:10.1128/JB.00191-07

Functional Incorporation of Chimeric *b* Subunits into F_1F_o ATP Synthase[▽]

Shane B. Claggett,[1] Tammy Bohannon Grabar,[1] Stanley D. Dunn,[2] and Brian D. Cain[1]*

Department of Biochemistry and Molecular Biology, University of Florida, Gainesville, Florida 32605,[1] and Department of Biochemistry, University of Western Ontario, London, Ontario, Canada N6A 5C1[2]

Received 5 February 2007/Accepted 15 May 2007

F_1F_o ATP synthases function by a rotary mechanism. The enzyme's peripheral stalk serves as the stator that holds the F_1 sector and its catalytic sites against the movement of the rotor. In *Escherichia coli*, the peripheral stalk is a homodimer of identical *b* subunits, but photosynthetic bacteria have open reading frames for two different *b*-like subunits thought to form heterodimeric *b*/*b′* peripheral stalks. Chimeric *b* subunit genes have been constructed by substituting sequence from the *Thermosynechococcus elongatus b* and *b′* genes in the *E. coli uncF* gene, encoding the *b* subunit. The recombinant genes were expressed alone and in combination in the *E. coli* deletion strain KM2 (Δ*b*). Although not all of the chimeric subunits were incorporated into F_1F_o ATP synthase complexes, plasmids expressing either chimeric $b_{E39\text{-}I86}$ or $b'_{E39\text{-}I86}$ were capable of functionally complementing strain KM2 (Δ*b*). Strains expressing these subunits grew better than cells with smaller chimeric segments, such as those expressing the $b'_{E39\text{-}D53}$ or $b_{L54\text{-}I86}$ subunit, indicating intragenic suppression. In general, the chimeric subunits modeled on the *T. elongatus b* subunit proved to be more stable than the *b′* subunit in vitro. Coexpression of the $b_{E39\text{-}I86}$ and $b'_{E39\text{-}I86}$ subunits in strain KM2 (Δ*b*) yielded F_1F_o complexes containing heterodimeric peripheral stalks composed of both subunits.

F_1F_o ATP synthases generate the majority of ATP consumed by living organisms and are found in the plasma membrane of bacteria, the inner membrane of mitochondria, and the thylakoid membrane of chloroplasts. All F_1F_o ATP synthases function by a conserved mechanism in which the electrochemical energy of a proton or sodium gradient is harnessed to synthesize ATP from ADP and inorganic phosphate (for reviews, see references 3, 22, and 30). In *Escherichia coli* the membrane-embedded F_o sector housing the proton channel is composed of three different subunits in the stoichiometry ab_2c_{10}. The F_1 sector consists of five subunits in the stoichiometry $\alpha_3\beta_3\gamma\delta\varepsilon$. F_1F_o ATP synthase functions as a rotary motor. The translocation of protons through the F_o channel results in movement of the rotor stalk consisting of the $c_{10}\gamma\varepsilon$ subunits relative to the remainder of the complex. The rotation drives ATP synthesis via conformation shifts in the catalytic sites located at the interfaces between the $\alpha_3\beta_3$ subunits. The $\alpha_3\beta_3$ subunits are held in place against the rotation of the rotor stalk by the peripheral stalk composed of the $b_2\delta$ subunits.

In *E. coli*, the peripheral stalk is an extended homodimer of identical *b* subunits (2, 9, 35). Each *b* subunit has an N-terminal transmembrane domain and stretches the length of the F_1F_o complex, making direct contact with the δ subunit perched atop and to one side of the F_1 sector (8, 19). Three distinct functional domains have been defined within the hydrophilic portion of the *b* subunits (26). First, the tether domain roughly corresponds to the segment between the surface of the membrane and a position beneath the F_1 sector. Both large deletions and insertions can be readily accommodated in this domain (32, 34), and functional F_1F_o complexes with peripheral stalks containing two *b* subunits with tether domains differing in length have been engineered (15). The dimerization domain extends up into one of the noncatalytic αβ interfaces in F_1 (18). This section is essential and sufficient for the formation of a dimer of the soluble form of the *b* subunit (26). A high-resolution structure of a polypeptide modeling the dimerization domain from amino acids 62 to 122 revealed a linear α-helix (6). Recent analysis of disulfide cross-link formation within the *b* subunit dimerization domains suggested a right-handed coiled-coil arrangement (5). The C-terminal F_1 binding domain is required for interaction of the peripheral stalk and F_1 (1, 19). The structure of the soluble portions of the peripheral stalk from bovine mitochondrial F_1F_o ATP synthase was recently solved by crystallography and showed a stalk with three different subunits that formed an extended curving subcomplex (7).

In contrast, the peripheral stalks found in chloroplast F_1F_o ATP synthase consist of two different *b*-like polypeptides, named subunits I and II, that form a heterodimer (27). Some eubacteria, encompassing photosynthetic bacteria but including some other species, also have genes encoding two *b*-like subunits designated *b* and *b′*. Both polypeptides have been shown to be present in purified ATP synthase from *Aquifex aeolicus* (25). The general expectation that *b* and *b′* form a heterodimer has been supported by studies of expressed hydrophilic domains of the subunits from the cyanobacterium *Synechocystis* sp. strain PCC6803 (10). Sedimentation analyses showed that the predominant species present in equimolar mixtures of the two polypeptides had a molecular weight expected for the heterodimer, whereas the individual polypeptides gave molecular weights corresponding to monomers. Heterodimer formation was also supported by chemical cross-linking. To our knowledge, however, it has never been demonstrated that only heterodimeric stalks are formed within the enzyme, or, alternatively, whether b_2 and b'_2 homodimeric stalks might also exist and support function.

* Corresponding author. Mailing address: Department of Biochemistry and Molecular Biology, Box 100245, University of Florida, Gainesville, FL 32610. Phone: (352) 392-6473. Fax: (352) 392-2953. E-mail: bcain@biochem.med.ufl.edu.

▽ Published ahead of print on 25 May 2007.

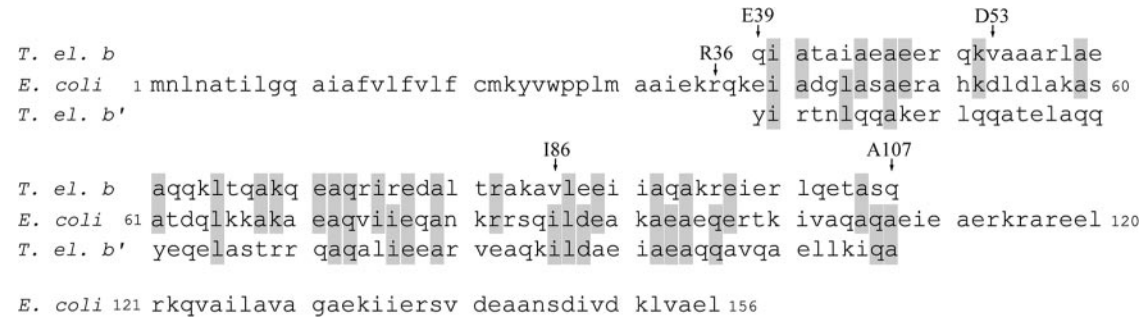

FIG. 1. Alignment of the *E. coli b* subunit sequence with the sequences of the *T. elongatus b* and *b′* subunits over the E39-to-A107 region. Identical amino acids are shaded, and the positions mentioned in the text are labeled.

Thermosynechococcus elongatus BP-1 is a thermophilic cyanobacterium whose entire genome has been sequenced (21). Although little is known about the F_1F_o ATP synthase of *T. elongatus* other than the sequence information, it has been used as a model organism for the study of photosynthesis (23) and circadian rhythms (24). *T. elongatus* BP-1 has genes encoding both *b* and *b′* subunits, and these genes share a relatively high degree of sequence identity with the *Synechocystis* genes. There are approximately 50% identity and 70% similarity in the deduced amino acid sequences of both *b* and *b′* genes between the two organisms. Therefore, it seems reasonable to assume that the *b* and *b′* subunits of *T. elongatus* will preferentially form heterodimeric peripheral stalks.

In this work we have generated chimeric *b* subunits by replacing segments of the *E. coli uncF* gene, encoding the *b* subunit, with either *b* or *b′* sequence based on the *T. elongatus* genes (Fig. 1). The recombinant subunit genes were expressed alone and in combination in an *E. coli uncF* deletion strain. Although some of the chimeric subunits failed to assemble into F_1F_o ATP synthase complexes, others were incorporated and were capable of functional complementation of the deletion strain. Expression of chimeric subunits to form only homodimeric stalks was in some cases sufficient for activity. When expressed together, the *b* and *b′* chimeric subunits readily formed heterodimeric peripheral stalks in F_1F_o ATP synthase complexes.

MATERIALS AND METHODS

Bacterial strains and growth conditions. *E. coli* strain KM2 (Δ*b*), which carries a chromosomal deletion of the *uncF* (*b* subunit) gene, and strain 1100 ΔBC (Δ*unc*), lacking the entire *unc* operon, were used as the host strains (17). Cells were grown on minimal A medium supplemented with succinate (0.2%, wt/vol) to determine enzyme viability. Cells harvested for membrane preparations were grown in Luria broth supplemented with glucose (0.2%, wt/vol) and isopropyl-1-thio-β-D-galactopyranoside (IPTG; 40 μg/ml). IPTG, ampicillin (100 μg/ml), and chloramphenicol (25 μg/ml) were added as needed. All cells were grown at 37°C unless otherwise noted.

Expression plasmid construction. Ten plasmids were constructed for expression of chimeric *E. coli*/*T. elongatus b* or *b′* subunits (Table 1). Five of these plasmids expressed a chimeric *b* subunit with a histidine tag (his_6) on the amino terminus, and five expressed a chimeric *b′* subunit with a V5 tag (GKPIPNPLL GLDST) on the carboxyl terminus. The plasmids expressing chimeric *b* and *b′* subunits were constructed using expression plasmids pTAM37 (b_{his}; Cm^r) and pTAM46 (b_{V5}; Ap^r), respectively (15). Sections of nucleotide sequences of the *uncF* (*b* subunit) gene from *E. coli* codons E39 to A107 were replaced with the homologous *T. elongatus b* and *b′* sequences. This was accomplished by cassette site-directed mutagenesis essentially as described previously (16). The *E. coli* sequence was replaced in three steps using four restriction sites located within the *uncF* gene: SnaBI, which cuts at nucleotide 72; PpuMI, cutting at nucleotide 156; XbaI, at nucleotide 258; and SapI, at nucleotide 347 (Table 2). The mutated sequences were E39 to D53 for the SnaBI and PpuMI sites, L54 to I86 for the PpuMI and XbaI sites, and L87 to A107 for the XbaI and SapI sites. The native cysteine in the *b* subunit was mutated to a serine (C25S) in all constructs, and the chimeric *b* subunit genes were confirmed by direct nucleotide sequencing.

Preparation of membranes. Membranes were prepared using the method of Caviston et al. (4). Bacterial cells were harvested upon reaching an optical density at 600 nm of approximately 1.0. The cells were collected by centrifugation in a Du Pont Sorvall RC-5B Superspeed centrifuge with a GSA rotor at 10,000 × *g* for 10 min and were resuspended in TM buffer (50 mM Tris-HCl [pH 7.5], 10 mM $MgSO_4$). DNase I was added to a final concentration of 10 μg/ml, and the cells were broken by passing them twice through a French pressure cell at 14,000 lb/in^2. Two sequential centrifugation steps in the same Sorvall centrifuge with an SS-34 rotor at 10,000 × *g* for 10 min were carried out to remove unbroken cells and debris. Membrane vesicles were recovered by centrifugation in a Beckman-Coulter Optima LE-80K ultracentrifuge with a 70.1 Ti rotor at 150,000 × *g* for 1.5 h. Membranes were washed by resuspending them in TM buffer using a glass homogenizer and a Teflon pestle and then centrifuging them again in the Beckman centrifuge for 1 h. The washed membranes were suspended again with the homogenizer in a final volume of 1 ml TM buffer, and the protein concentration was determined using the bicinchoninic acid method (31).

Activity assays. The ATP hydrolysis activity of membrane samples was determined using the acid molybdate method to monitor the release of inorganic phosphate as previously described (32). Reactions were carried out with 60 μg of protein suspended in 4 ml of reaction buffer (50 mM Tris-HCl [pH 7.5], 1 mM $MgCl_2$) at 37°C unless otherwise specified. Lauryl dimethylamine oxide (LDAO) stimulation of ATP hydrolysis activity was determined by adding LDAO to the

TABLE 1. Plasmids used in this study

Plasmid	Gene product[a]	Antibiotic resistance[b]	Source or reference
pBR322	Δ*b*	Ap	New England Biolabs
pTAM37	b_{his}	Cm	15
pTAM46	b_{V5}	Ap	15
pSBC56	$b_{E39\text{-}D53,\ his}$	Cm	This study
pSBC57	$b'_{E39\text{-}D53,\ V5}$	Ap	This study
pSBC58	$b_{L54\text{-}I86,\ his}$	Cm	This study
pSBC76	$b'_{L54\text{-}I86,\ V5}$	Ap	This study
pSBC97	$b_{E39\text{-}I86,\ his}$	Cm	This study
pSBC98	$b'_{E39\text{-}I86,\ V5}$	Ap	This study
pSBC94	$b_{L54\text{-}A107,\ his}$	Cm	This study
pSBC79	$b'_{L54\text{-}A107,\ V5}$	Ap	This study
pSBC95	$b_{E39\text{-}A107,\ his}$	Cm	This study
pSBC96	$b'_{E39\text{-}A107,\ V5}$	Ap	This study

[a] his, six-histidine epitope tag at the amino terminus; V5, epitope tag with the sequence GKPIPNPLLGLDS appended to the carboxyl terminus. The replaced regions are designated by the first and last *E. coli* amino acids that were replaced with *T. elongatus* sequence.

[b] Ap, ampicillin; Cm, chloramphenicol.

TABLE 2. Synthetic oligonucleotides used in this study

Oligonucleotide pair (gene)	Annealed oligonucleotide	Sequence[a]
TG1/2[b] ($b_{E39\text{-}D53}$)	TG1	5′-GTATGGCCGCCACTGATGGCAGCCATCGAAAAACGTCAAAAACAGATCGCTACTGC TATCGCTGAAGCTGAAGAACGTCAGAAG-3′
	TG2	3′-CATACCGGCGGTGACTACCGTCGGTAGCTTTTTGCAGTTTTTGTCTAGCGATGACGA TAGCGACTTCGACTTCTTGCAGTCTTCCTG-5′
TG3/4 ($b'_{E39\text{-}D53}$)	TG3	5′-GTATGGCCGCCACTGATGGCAGCCATCGAAAAACGTCAAAAATACATCCGTACTAA CCTGCAGCAGGCTAAAGAACGTCTGCAGCAG-3′
	TG4	3′-CATACCGGCGGTGACTACCGTCGGTAGCTTTTTGCAGTTTTTATGTAGGCATGATTG GACGTCGTCCGATTTCTTGCAGACGTCGTCCTG-5′
TG13/10[c] ($b_{L54\text{-}I86}$)	TG13	5′-GACGTTGCTGCTGCTCGTCTGGCTGAAGCTCAGCAGAAACTGACTCAGGCTAAACA GGAGGCTCAGCGTATCCGTGAAGATGCTCTGACTCGTGCTAAAGCTGTT-3′
	TG10	3′-CAACGACGACGAGCAGACCGACTTCGAGTCGTCTTTGACTGAGTCCGATTTGTCCTC CGAGTCGCATAGGCACTTCTACGAGACTGAGCACGATTTCGACAAGATC-5′
TG14/12 ($b'_{L54\text{-}I86}$)	TG14	5′-GACGCTACTGAACTGGCTCAGCAGTACGAACAGGAGCTGGCTTCCACTCGTCGTCA GGCTCAGGCTCTGATCGAAGAAGCTCGTGTTGAAGCTCAGAAAATT-3′
	TG12	3′-CGATGACTTGACCGAGTCGTCATGCTTGTCCTCGACCGAAGGTGAGCAGCAGTCCG AGTCCGAGACTAGCTTCTTCGAGCACAACTTCGAGTCTTTTAAGATC-5′
SC39/40[d] ($b_{L87\text{-}A107}$)	SC39	5′-CTAGAAGAAATTATTGCTCAGGCTAAACGTGAAATTGAACGTCTGCAGGAGACCGC TAGCCAGGAAATTGAAGCCGAGCGTAAACGTGC-3′
	SC40	3′-TTCTTTAATAACGAGTCCGATTTGCACTTTAACTTGCAGACGTCCTCTGGCGATCGG TCCTTTAACTTCGGCTCGCATTTGCACGGGC-5′
SC43/44 ($b'_{L87\text{-}A107}$)	SC43	5′-CTAGATGCGGAAATTGCGGAAGCGCAGCAGGCGGTCCAGGCGGAGCTCTTGAAAA TTCAGGCGGAAATTGAAGCCGAGCGTAAACGTGC-3′
	SC44	3′-TACGCCTTTAACGCCTTCGCGTCGTCCGCCAGGTCCGCCTCGAGAACTTTTAAGTCC GCCTTTAACTTCGGCTCGCATTTGCACGGGC-5′
SC45/46 (b_{C25S} + AflIII)	SC45	5′-CTGTTCGTTCTGTTCTCCATGAAGTACGTGTGGCCGCC-3′
	SC46	3′-GACAAGCAAGACAAGAGGTACTTCATGCACACCGGCGG-5′
SC59/60[e] (b_{-D} + SacII)	SC59	5′-ACTGCTATCGCTGAAGCTGAAGAACGTCAGAAGGTTGCCGCGGCTCGTCTGGCTGA AGCTCAGCAGAAACTG-3′
	SC60	3′-TGACGATAGCGACTTCGACTTCTTGCAGTCTTCCAACGGCGCCGAGCAGACCGACT TCGAGTCGTCTTTGAC-5′
SC61/62 (b'_{-D} + NheI)	SC61	5′-ACTAACCTGCAGCAGGCTAAAGAACGTCTGCAGCAGGCTACTGAGCTAGCTCAGCA GTACGAACAGGAGCTGGCT-3′
	SC62	3′-TGATTGGACGTCGTCCGATTTCTTGCAGACGTCGTCCGATGACTCGATCGAGTCGTC ATGCTTGTCCTCGACCGA-5′
SC53/54 (b + SpeI)	SC53	5′-GCTGCTAACAGCGACATCGTGGATAAACTAGTCGCTGAACTGTAAGGAGGGAGG-3′
	SC54	3′-CGACGATTGTCGCTGTAGCACCTATTTGATCAGCGACTTGACATTCCTCCCTCC-5′
SC57/58 (b + SnaBI)	SC57	5′-CTGTTCGTTCTGTTCTCCATGAAGTACGTATGGCCGCC-3′
	SC58	3′-GACAAGCAAGACAAGAGGTACTTCATGCATACCGGCGG-5′
TB38/39 (b_{V5} + SacI)	TB38	5′-CGTGGATAAACTTGTCGCTGAGCTC**GGTAAACCGATCCCGAACCCGCTGCTGGGTCTG GACTCTACC**TAAGGAGGGAGGGGCTGATG-3′
	TB39	3′-GCACCTATTTGAACAGCGACTCGAG**CCATTTGGCTAGGGCTTGGGCGACGACCCAGAC CTGAGATGG**ATTCCTCCCTCCCCGACTAC-5′

[a] Added restriction sites are underlined, and the V5 epitope tag is boldfaced.
[b] Oligonucleotides TG1/2 (*b*) and TG3/4 (*b′*) were used to replace DNA between restriction sites SnaBI and PpuMI.
[c] Oligonucleotides TG13/10 (*b*) and TG14/12 (*b′*) were used to replace DNA between restriction sites PpuMI and XbaI.
[d] Oligonucleotides SC39/40 (*b*) and SC43/44 (*b′*) were used to replace DNA between restriction sites XbaI and SapI.
[e] Oligonucleotides SC59/60 (*b*) and SC61/62 (*b′*) were used to remove an unwanted aspartic acid between the E39-to-D53 and L54-to-I86 regions.

ATP hydrolysis reaction mixture at a final concentration of 0.5% as previously described (13). ATP- and NADH-driven proton pumping assays were conducted by adding 500 μg of membrane protein to 3.5 ml reaction buffer (50 mM morpholinepropanesulfonic acid [MOPS; pH 7.3], 10 mM $MgCl_2$) and monitoring the fluorescence quenching of 9-amino-6-chloro-2-methoxyacridine (ACMA) as previously described (33). Fluorescence quenching was detected using two spectrofluorometers, either a Perkin-Elmer LS-3B or a Photon Technologies International QuantaMaster 4.

Trypsin digestion. The incorporation of chimeric *b* subunits into intact F_1F_o ATP synthase complexes was detected by the digestion of membrane samples with trypsin to degrade unincorporated *b* subunit as previously described (34). The *b* subunits were digested by bringing a total of 0.1 mg of membrane protein to a volume of 90 μl using TM buffer and adding 10 μl of 2-mg/ml trypsin to start the reaction. Aliquots containing 10 μg of digested protein were removed at 1, 2, 3, 4, 6, 8, and 16 h, and the reaction was stopped by the addition of 2 μl of 10-mg/ml trypsin inhibitor from *Glycine max* (soybean; Sigma-Aldrich). For long digestions, additional trypsin was added at 3, 6, and 8 h to compensate for the estimated activity loss of 25%/3 h. The samples were studied by Western blot analysis with 1 μg of each sample loaded per lane. The presence of heterodimeric peripheral stalks in intact F_1F_o complexes was examined by the digestion of 0.5 mg of membrane protein in a reaction volume of 100 μl. The entire reaction was stopped by the addition of 30 μl of 10-mg/ml trypsin inhibitor, and the product was purified over a nickel resin and analyzed by Western blot analysis (see below).

Nickel resin purification. Membrane samples were solubilized and purified over a high-capacity nickel chelate affinity matrix (Ni-CAM), purchased from Sigma, to selectively retain F_1F_o ATP synthase complexes containing at least one histidine tag as previously described (15). A total of 0.5 mg of membrane protein was brought up to a volume of 150 μl with a final concentration of 1 mM imidazole, 0.2 M NaCl, and 0.2% Tegamine oxide WS-35. The solubilized membrane protein was purified over 75 μl of Ni-CAM resin essentially as described by the manufacturer. The resin was incubated with the membrane protein for 10 min and then washed five times with wash buffer (50 mM Na_2PO_4 [pH 8.0], 0.2 M NaCl, 1 mM imidazole, 0.2% Tegamine oxide WS-35). Any bound protein was eluted in elution buffer (50 mM Na_2PO_4 [pH 8.0], 0.3 M NaCl, 250 mM imidazole) by incubating the resin twice for 10 min with 125 μl of elution buffer. The eluted protein was concentrated using a Microcon YM-10 centrifugal filter device, and the volume of the eluant was estimated by weight.

TABLE 3. Growth properties and ATPase activities in cells expressing chimeric subunits

Strain/plasmid(s)	Gene product(s)	Growth on succinate[a]	ATP hydrolysis activity[b]	
			Without LDAO	With 0.5% LDAO[c]
KM2/pTAM37/pTAM46	b_{his}/b_{V5}	+++	0.62 ± 0.04	1.21 ± 0.01
KM2/pBR322	Δb	−	0.13 ± 0.02	0.22 ± 0.01
KM2/pSBC56	$b_{E39\text{-}D53,\ his}$	+	0.58 ± 0.03	1.27 ± 0.07
KM2/pSBC57	$b'_{E39\text{-}D53,\ V5}$	−	0.20 ± 0.01	0.18 ± 0.04
KM2/pSBC56/pSBC57	$b_{E39\text{-}D53,\ his}/b'_{E39\text{-}D53,\ V5}$	+	0.61 ± 0.02	1.26 ± 0.06
KM2/pSBC58	$b_{L54\text{-}I86,\ his}$	−	0.42 ± 0.01	0.71 ± 0.02
KM2/pSBC76	$b'_{L54\text{-}I86,\ V5}$	+++	0.22 ± 0.01	0.31 ± 0.02
KM2/pSBC58/pSBC76	$b_{L54\text{-}I86,\ his}/b'_{L54\text{-}I86,\ V5}$	+++	0.47 ± 0.03	0.76 ± 0.06
KM2/pSBC97	$b_{E39\text{-}I86,\ his}$	+	0.50 ± 0.04	0.87 ± 0.08
KM2/pSBC98	$b'_{E39\text{-}I86,\ V5}$	++	0.19 ± 0.01	0.26 ± 0.01
KM2/pSBC97/pSBC98	$b_{E39\text{-}I86,\ his}/b'_{E39\text{-}I86,\ V5}$	++	0.49 ± 0.04	0.88 ± 0.02
KM2/pSBC94	$b_{L54\text{-}A107,\ his}$	−	0.22 ± 0.01	0.30 ± 0.01
KM2/pSBC79	$b'_{L54\text{-}A107,\ V5}$	−	0.15 ± 0.01	0.44 ± 0.03
KM2/pSBC94/pSBC79	$b_{L54\text{-}A107,\ his}/b'_{L54\text{-}A107,\ V5}$	−	0.23 ± 0.03	0.29 ± 0.03
KM2/pSBC95	$b_{E39\text{-}A107,\ his}$	−	0.12 ± 0.03	0.34 ± 0.01
KM2/pSBC96	$b'_{E39\text{-}A107,\ V5}$	−	0.12 ± 0.02	0.16 ± 0.03
KM2/pSBC95/pSBC96	$b_{E39\text{-}A107,\ his}/b'_{E39\text{-}A107,\ V5}$	−	0.14 ± 0.03	0.37 ± 0.02

[a] Symbols: +++, wild-type growth; ++, colonies smaller than wild type; +, small-colony formation; −, no growth.
[b] Reported in μmol of P_i/mg of membrane protein/min.
[c] Used to release F_1 from the inhibitory effect of F_o.

Western blotting. Proteins were separated on a 15% sodium dodecyl sulfate-polyacrylamide gel, and Western blotting was performed as described previously (14). The primary and secondary antibodies used here were the anti-*b* subunit antibody (a gift from G. Deckers-Hebestreit) and the anti-V5 antibody (Invitrogen). The presence of bound secondary antibody was detected by chemiluminescence using Amersham Biosciences' ECL Plus Western blotting detection system.

RESULTS

Complementation analysis. For complementation studies, plasmids pTAM37 (b_{his}; Cm^r) and pTAM46 (b_{V5}; Ap^r) were transformed into deletion strain KM2 (Δb) to serve as positive controls (15). The *b* subunits expressed by these plasmids were equipped with different epitope tags to facilitate the detection of heterodimeric peripheral stalks. The epitope tags had very little effect on enzyme activity. Ten additional plasmids have been constructed to express chimeric subunits in which parts of the tether and dimerization domains of the *E. coli b* subunit have been replaced with the homologous *b* or *b′* segments from *T. elongatus* (Fig. 1). This organism was chosen in an attempt to increase the stability of the chimeric constructs. The amino and carboxyl boundaries of the substituted region were selected to avoid disturbing the environment of the critical R36 residue and to prevent disruption of essential interactions between the peripheral stalk and F_1. The abilities of these plasmids to complement deletion strain KM2 (Δb) were studied by growth on minimal A medium supplemented with succinate (Table 3). Plasmids that contained *T. elongatus b* or *b′* sequence between either D54 and A107 or E39 and A107 were unable to complement strain KM2. Similarly, KM2/pSBC57 ($b'_{E39\text{-}D53,\ V5}$) failed to grow on succinate medium, but a weakly positive result was obtained with strain KM2/pSBC56 ($b_{E39\text{-}D53,\ his}$). Much more impressive complementation was obtained with strain KM2/pSBC76 ($b'_{L54\text{-}I86,\ V5}$), but KM2/pSBC58 ($b_{L54\text{-}I86,\ his}$) did not grow. Interestingly, colony formation was in evidence when either chimeric $b_{E39\text{-}I86,\ his}$ or $b'_{E39\text{-}I86,\ V5}$ subunits were expressed.

Stability of F_1F_o complexes. In order to detect the expression of the recombinant *b* subunits and their incorporation into membranes, the presence of *b* subunit proteins was studied by Western blot analysis. The experiments were performed on membrane samples prepared from cells expressing chimeric *b* or *b′* subunits either alone or together (Fig. 2). The Western blots were probed with a polyclonal antibody against the *b* subunit or a monoclonal antibody against the V5 epitope tag. The *E. coli* anti-*b* subunit antibody recognized the chimeric b_{his} subunits in membranes prepared from KM2 cells expressing the $b_{E39\text{-}D53,\ his}$, $b_{L54\text{-}I86,\ his}$, or $b_{E39\text{-}I86,\ his}$ subunit. Although b'_{V5} subunits appeared to be present at lower levels than the controls, these subunits were detected by the anti-V5 antibody in membranes prepared from cells expressing $b'_{E39\text{-}D53,\ V5}$, $b'_{L54\text{-}I86,\ V5}$, or $b'_{E39\text{-}I86,\ V5}$ subunits. The chimeric *b′* subunits were not detectable with the antibody against the *E. coli b* subunit. The first indication of a likely interaction between chimeric *b* and *b′* subunits within an F_1F_o complex was the observation that the $b'_{E39\text{-}D53,\ V5}$ subunit seemed to be stabilized in the membrane in the presence of the $b_{E39\text{-}D53,\ his}$ subunit (Fig. 2, E39-D53, lanes 4 and 5). The absence of signals for the chimeric *b* or *b′* subunit with *T. elongatus* sequence from D54 to A107 or from E39 to A107 with either antibody suggested that the chimeric segment could not be extended further toward the C terminus. These proteins apparently failed to be stably incorporated into the membranes and were degraded.

Membrane-associated ATP hydrolysis was determined for KM2 cells expressing chimeric *b* and *b′* subunits (Table 3).

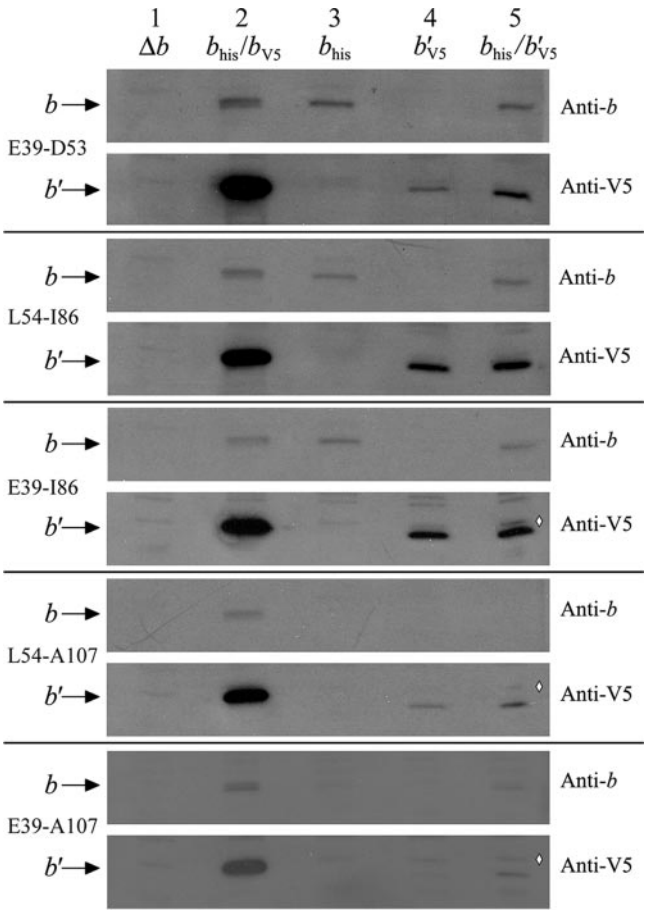

FIG. 2. Immunoblot of membranes prepared from *E. coli* strain KM2 (Δ*b*) expressing chimeric *b* subunits. Aliquots of membrane proteins (1 μg) were separated on 15% sodium dodecyl sulfate-polyacrylamide gels and transferred to nitrocellulose membranes as previously described (14). The presence of the *b* subunit was detected using both a polyclonal antibody raised against the *b* subunit and an antibody against the V5 epitope tag appended to the carboxyl terminus of the chimeric *b′* subunits. The position of the *b* subunit band and the region that was replaced with *T. elongatus* sequence are indicated on the left and the primary antibody on the right. Membrane samples were loaded as follows: lane 1, negative control KM2/pBR322 (Δ*b*); lane 2, positive control KM2/pTAM37/pTAM46 (b_{his}/b_{V5}); lane 3, chimeric b_{his} subunits; lane 4, chimeric b'_{V5} subunits; lane 5, coexpression of chimeric b_{his} and b'_{V5} subunits. The commercial anti-V5 antibody gave a much stronger signal than the polyclonal anti-*b* subunit antibody and also detected an extra band running near the level of the *b* subunit, indicated in lane 5 by a white diamond (◇).

Since the *b* subunit is required for association of the F_1 complex with the F_o complex, membrane-associated ATPase activity can in some cases be used as an indirect indication of the relative amounts of intact F_1F_o complexes stably incorporated into the membrane. As expected, only very low levels of ATP hydrolysis were observed in membranes prepared from cells expressing chimeric *b* or *b′* subunits with *T. elongatus* sequence replacing L54 to A107 or E39 to A107, a result that correlated well with failed complementation tests and negative Western blotting results. In contrast, substantial ATP hydrolysis activity was seen with all chimeric *b* subunits with replacements between E39 and D53, L54 and I86, or E39 and I86. Strangely, this was not true of the chimeric *b′* subunits. Membranes prepared from KM2/pSBC57 ($b'_{E39\text{-}D53,\ V5}$), KM2/pSBC76 ($b'_{L54\text{-}I86,\ V5}$), and KM2/pSBC98 ($b'_{E39\text{-}I86,V5}$) all had very little membrane-associated ATP hydrolysis activity. Given that two of the strains had solidly positive complementation test results, it was necessary to look into this issue further. We successfully reproduced the complementation analysis and then sequenced plasmid DNA prepared from the colonies grown on succinate minimal medium. The *uncF* (*b* subunit) genes in these plasmids retained the designed chimeric *b* subunit gene and carried no other mutations. A recent publication suggested that a cold-stabilized form of the complex had a significant lag in ATP hydrolysis activity (12). Therefore, ATP hydrolysis was carefully reexamined under conditions that would account for a potential lag, and results essentially identical to those shown in Table 3 were obtained.

Another possibility was that the chimeric *b′* subunits inhibited F_1F_o ATP hydrolysis. LDAO releases F_1 from the influence of F_o-associated mutations (13) and promotes release of the inhibitory ε subunit (11), so determination of ATP hydrolysis activity in the presence of LDAO yields a value reflecting the total F_1 present in a membrane sample. The amount of LDAO stimulation observed indicated that the KM2/pSBC76 ($b'_{L54\text{-}I86,\ V5}$) and KM2/pSBC98 ($b'_{E39\text{-}I86,V5}$) samples had only minimal F_1 bound. Therefore, it seems that although the two strains grew well, indicating abundant F_1F_o ATP synthase function in vivo, the F_1F_o complexes were not stable and were lost during membrane preparation. The reduced levels of b'_{V5} subunits seen during the Western blot analysis (Fig. 2) lent further support to this interpretation.

Coupled F_1F_o activity. ATP-driven proton pumping in membrane vesicles was used to detect coupled activity in F_1F_o complexes with chimeric peripheral stalks (Fig. 3). Acidification of inverted membrane vesicles was monitored by fluorescence quenching of ACMA. All membrane samples had strong ACMA quenching upon addition of NADH, confirming that the membrane vesicles were intact and closed (data not shown). KM2/pSBC57 ($b'_{E39\text{-}D53,\ V5}$) membranes showed no proton pumping activity, but strong fluorescence quenching was seen in KM2/pSBC56 ($b_{E39\text{-}D53,\ his}$) membranes (Fig. 3A). KM2/pSBC58 ($b_{L54\text{-}I86,\ his}$) and KM2/pSBC76 ($b'_{L54\text{-}I86,\ V5}$) membranes showed low but detectable levels of ATP-driven proton pumping (Fig. 3B). No activity was observed in membranes prepared from either KM2/pSBC94 ($b_{L54\text{-}A107,\ his}$) or KM2/pSBC79 ($b'_{L54\text{-}A107,\ V5}$) (Fig. 3D). Membranes from KM2/pSBC95 ($b_{E39\text{-}A107,\ his}$) showed limited fluorescence quenching under our most sensitive assay conditions (data not shown). The most interesting results were obtained by looking at the E39-to-I86 chimeric subunits (Fig. 3C). Coexpression of the chimeric $b_{E39\text{-}I85,\ his}$ and $b'_{E39\text{-}I86,\ V5}$ subunits reproducibly yielded higher proton pumping activity than expression of either of the individual subunits alone. Moreover, the initial rate of fluorescence quenching was substantially higher in the KM2/pSBC97/pSBC98 ($b_{E39\text{-}I86,\ his}/b'_{E39\text{-}I86,\ V5}$) membranes (Table 4). These results might have reflected either the additive activity from the $(b_{E39\text{-}I86,\ his})_2$ and $(b'_{E39\text{-}I86,\ V5})_2$ homodimeric complexes or, more likely, the presence of F_1F_o complexes containing $b_{E39\text{-}I86,\ his}/b'_{E39\text{-}I86,\ V5}$ heterodimeric complexes.

Detection of heterodimers. In order to detect F_1F_o complexes with heterodimeric peripheral stalks, a nickel resin pu-

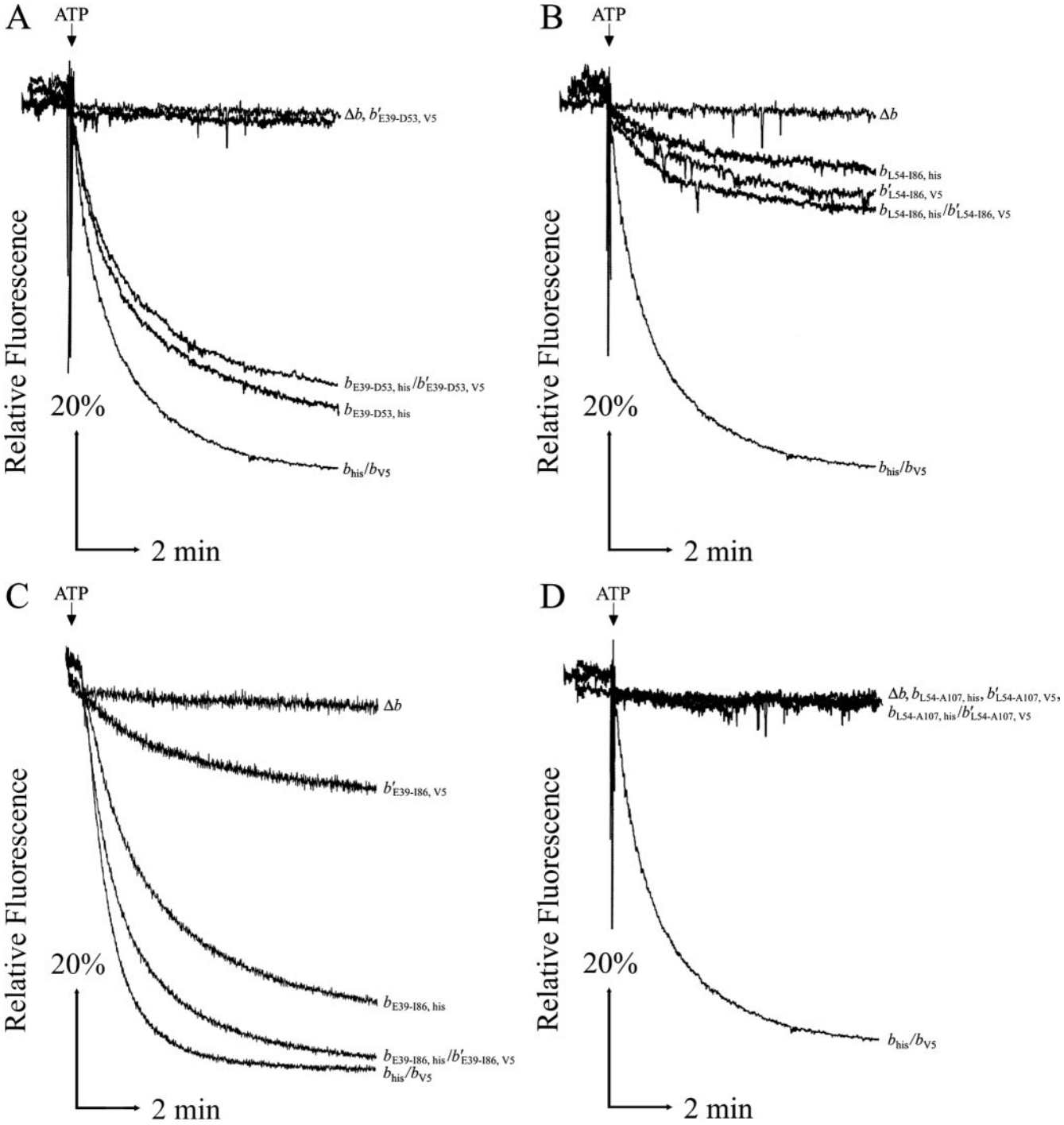

FIG. 3. ATP-driven energization of membrane vesicles prepared from KM2 (Δ*b*) cells expressing chimeric *b* subunits. Aliquots of membrane proteins (500 μg) were suspended in 3.5 ml assay buffer (50 mM MOPS [pH 7.3], 10 mM $MgCl_2$), and fluorescence quenching of ACMA was used to detect energization of membrane vesicles after the addition of ATP as previously described (33). Traces are plotted as relative fluorescence over time. The point where ATP was added is indicated above each graph, and chimeric subunits are given on the right. Each panel shows traces of membranes from the negative control KM2/pBR322 (Δ*b*), the positive control KM2/pTAM37/pTAM46 (b_{his}/b_{V5}), and the *b* and *b′* chimeric subunits expressed individually and together. The chimeric subunits in the panels are as follows: E39 to D53 (A), L54 to I86 (B), E39 to I86 (C), and L54 to A107 (D). Traces were obtained using a Perkin-Elmer (A, B, and D) or Photon Technologies International (C) spectrofluorometer.

rification procedure developed previously in our lab (15) was used to examine membranes prepared from KM2/pSBC97/pSBC98 ($b_{E39\text{-}I86,\ his}/b'_{E39\text{-}I86,\ V5}$) (Fig. 4B, lanes 1 to 10). Four important controls were included in the experiment. To confirm that the resin was retaining only F_1F_o complexes containing the chimeric $b_{E39\text{-}I86,\ his}$ subunit, membranes prepared from KM2/pSBC98 ($b'_{E39\text{-}I86,\ V5}$) were processed, and no bands were observed using either the anti-*b* or the anti-V5

TABLE 4. Proton pumping rates of membranes prepared from cells expressing chimeric E39-to-I86 subunits

Strain/plasmid(s)	Gene product(s)	Final fluorescence (% of initial fluorescence)	Initial rate of decrease (%/min)
KM2/pTAM37/pTAM46	b_{his}/b_{V5}	22.2 ± 0.1	66.9 ± 0.6
KM2/pBR322	Δ*b*	91.7 ± 0.5	0.5 ± 0.2
KM2/pSBC97	$b_{E39\text{-}I86,\ his}$	34.5 ± 0.8	27 ± 2
KM2/pSBC98	$b'_{E39\text{-}I86,\ V5}$	76.0 ± 0.4	6.1 ± 1.1
KM2/pSBC97/pSBC98	$b_{E39\text{-}I86,\ his}/b'_{E39\text{-}I86,\ V5}$	28.0 ± 0.5	48 ± 3

antibody (Fig. 4B, lane 6). F_1F_o complexes from KM2/pSBC97 ($b_{E39\text{-}I86,\ his}$) were purified as a positive control to demonstrate that the resin retained histidine-tagged complexes and the anti-V5 antibody detected nothing in samples lacking a V5 epitope tag (lane 7). To address possible aggregation of F_1F_o complexes during sample preparation, membranes from strains KM2/pSBC97 ($b_{E39\text{-}I86,\ his}$) and KM2/pSBC98 ($b'_{E39\text{-}I86,\ V5}$) were mixed prior to solubilization. As expected, no band was observed using the anti-V5 antibody (lane 8). The positive control was nickel resin-purified F_1F_o complexes from KM2/pTAM37/pTAM46 (b_{his}/b_{V5}). The presence of complexes containing heterodimeric b_{his}/b_{V5} peripheral stalks was demonstrated by signals from both the anti-*b* and anti-V5 antibodies (lane 10). An essentially identical result was obtained using membranes from KM2/pSBC97/pSBC98 ($b_{E39\text{-}I86,\ his}/b'_{E39\text{-}I86,\ V5}$) (lane 9). The $b'_{E39\text{-}I86,\ V5}$ subunit could have been retained in the nickel resin-purified material only if it were part of an F_1F_o complex containing a $b_{E39\text{-}I86,\ his}$ subunit.

Trypsin digestion of membranes samples was used to confirm that the heterodimeric peripheral stalks were incorporated into intact F_1F_o complexes. A portion of the wild-type b_{V5} subunit remained resistant to degradation during an extended overdigestion with trypsin when expressed in the presence of the other F_1F_o ATP synthase genes (Fig. 4A, KM2 digestion). The same subunit was degraded when expressed alone in strain 1100 ΔBC (Δ*unc*), demonstrating that the incorporation of the *b* subunit into an intact F_1F_o complex protects the peripheral stalk from trypsin digestion. This result is consistent with what has been observed previously (34). Likewise, chimeric pSBC97/pSBC98 ($b_{E39\text{-}I86,\ his}/b'_{E39\text{-}I86,\ V5}$) subunits were partially protected by incorporation into F_1F_o complexes. A very small amount of b_{V5} subunit was detected in membranes exposed to trypsin in the absence of the rest of the

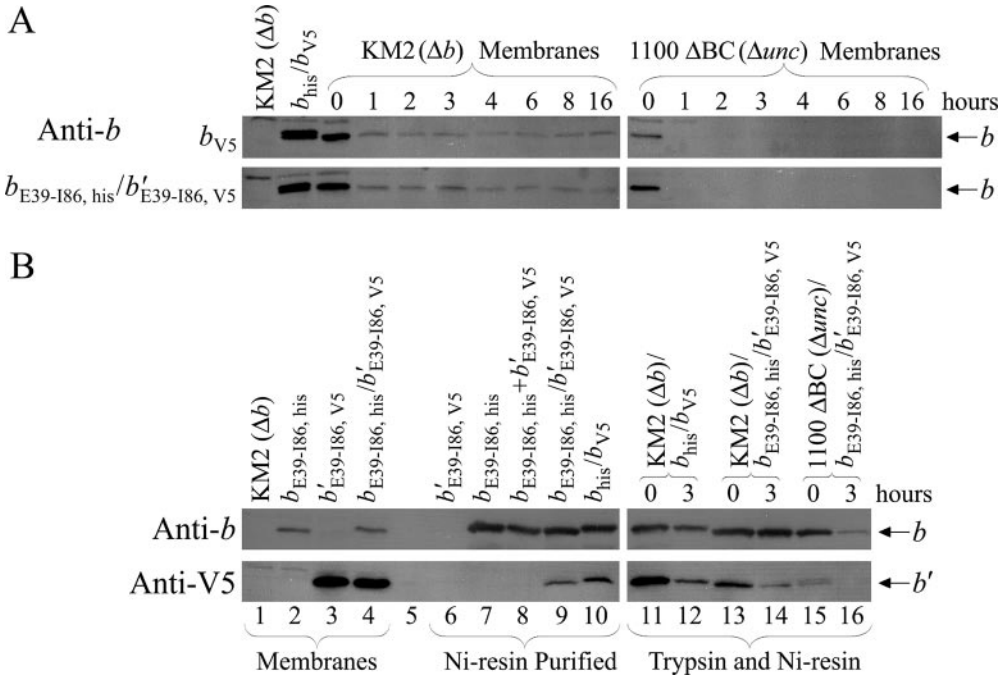

FIG. 4. Incorporation of heterodimeric peripheral stalks into F_1F_o ATP synthase complexes. (A) Trypsin digestion of either pTAM46 (b_{V5}) or pSBC97/pSBC98 ($b_{E39\text{-}I86,\ his}/b'_{E39\text{-}I86,\ V5}$) expressed in either KM2 (Δ*b*) or 1100 ΔBC (Δ*unc*) cells. The strains and expressed subunits are given on the figure. Proteolytic digestion and collection of aliquots were performed as described in Materials and Methods. Western blotting was performed, and blots were probed with an antibody against the *b* subunit as for Fig. 2. (B) Aliquots of membrane samples were solubilized and purified over Ni-CAM as previously described (15). Ten percent of the total eluant from the nickel resin purification was loaded in each lane of purified protein. Western blotting was performed with antibodies against both the *b* subunit and the V5 epitope tag. Membranes were loaded into lanes as follows: lanes 1 to 4, 1 μg of nonpurified membranes from KM2/pBR322 (Δ*b*), KM2/pSBC97 ($b_{E39\text{-}I86,\ his}$), KM2/pSBC98 ($b'_{E39\text{-}I86,\ V5}$), and KM2/pSBC97/pSBC98 ($b_{E39\text{-}I86,\ his}/b'_{E39\text{-}I86,\ V5}$), respectively; lane 5, intentionally left empty; lane 6, nickel resin negative control KM2/pSBC98 ($b'_{E39\text{-}I86,\ V5}$); lane 7, nickel resin positive control KM2/pSBC97 ($b_{E39\text{-}I86,\ his}$); lane 8, nickel resin aggregation control KM2/pSBC97 ($b_{E39\text{-}I86,\ his}$) plus KM2/pSBC98 ($b'_{E39\text{-}I86,\ V5}$); lane 9, purification of KM2/pSBC97/pSBC98 ($b_{E39\text{-}I86,\ his}/b'_{E39\text{-}I86,\ V5}$); lane 10, purification of heterodimer positive control KM2/pTAM37/pTAM46 (b_{his}/b_{V5}); lanes 11 and 12, purification of trypsin-digested KM2/pTAM37/pTAM46 (b_{his}/b_{V5}) at 0 and 3 h, respectively; lanes 13 and 14, purification of trypsin-digested KM2/pSBC97/pSBC98 ($b_{E39\text{-}I86,\ his}/b'_{E39\text{-}I86,\ V5}$) at 0 and 3 h, respectively; lanes 15 and 16, purification of trypsin-digested 1100 ΔBC/pSBC97/pSBC98 ($\Delta unc/b_{E39\text{-}I86,\ his}/b'_{E39\text{-}I86,\ V5}$) at 0 and 3 h, respectively.

complex using the higher-sensitivity antibody against the V5 epitope tag (data not shown). Nickel resin purification of samples digested with trypsin demonstrated that the heterodimeric peripheral stalks were incorporated into intact F_1F_o complexes (Fig. 4B, lanes 11 to 16). A band was seen using the anti-V5 antibody after 3 h of trypsin digestion for both the positive control KM2/pTAM37/pTAM46 (b_{his}/b_{V5}) and the chimeric KM2/pSBC97/pSBC98 ($b_{E39\text{-}I86,\ his}/b'_{E39\text{-}I86,\ V5}$) sample but not for the 1100 ΔBC/pSBC97/pSBC98 ($b_{E39\text{-}I86,\ his}/b'_{E39\text{-}I86,\ V5}$) sample. The $b'_{E39\text{-}I86,\ V5}$ subunit survived trypsin digestion and nickel resin purification as a component of a heterodimeric F_1F_o complex containing the $b_{E39\text{-}I86,\ his}$ subunit.

DISCUSSION

A series of plasmids have been constructed that were designed to express chimeric subunits such that portions of the tether and dimerization domains of the *E. coli* F_1F_o ATP synthase *b* subunit were replaced with homologous sequences from the *b* and *b′* subunits of the thermophilic cyanobacterium *T. elongatus*. The chimeric subunits with the largest successful *T. elongatus* segments had replacements spanning positions E39 to I86. The chimeric $b_{E39\text{-}I86}$ and $b'_{E39\text{-}I86}$ subunits each contained a total of 48 replaced amino acids, or almost one-third of the entire *b* subunit. Plasmids expressing either recombinant chimeric subunit were individually capable of genetic complementation of an *uncF* (*b* subunit) deletion strain. In addition to the homodimeric stalks formed by the expression of each subunit alone, coexpression of the $b_{E39\text{-}I86}$ and $b'_{E39\text{-}I86}$ subunits yielded readily detectable F_1F_o complexes with heterodimeric peripheral stalks. Attempts to extend the *T. elongatus* segment further toward the carboxyl terminus resulted in failure. The most logical interpretation was that critical interactions between the peripheral stalk and F_1 known to occur in this area of the *b* subunit (18, 20) were interrupted, leading to a general defect in assembly of the F_1F_o complex.

The secondary structure of the *b* subunit throughout the area under study here is thought to be an extended, linear α-helix (35). This has been confirmed by X-ray crystallography for the section covering amino acids 66 to 122 (6). In view of the properties of tether domain insertion and deletion mutants (15, 32, 34), one might have expected that any α-helical sequence substituted in the tether domain would be sufficient if the protein-protein contacts within F_o and F_1 were maintained. However, the $b'_{E39\text{-}D53,\ V5}$ chimeric subunit was fully defective. Extension of the chimeric region in the $b'_{E39\text{-}I86,\ V5}$ subunit resulted in formation of an active F_1F_o ATP synthase. Therefore, the structural defect induced by the substitutions in the $b'_{E39\text{-}D53}$ region was dramatically suppressed within the $b'_{E39\text{-}I86}$ subunit. The phenotype of the defective $b_{L54\text{-}I86,\ his}$ subunit was suppressed to a lesser degree in the $b_{E39\text{-}I86,\ his}$ subunit. The evidence suggests that there must be determinants throughout the E39-to-I86 section of the *b* subunit that act together to specify the structure of the peripheral stalk. The obvious interpretation is that multiple protein-protein interactions between the two *b* subunits likely provide these structural determinants. There is ample evidence for direct contacts within the dimerization domain (28, 29). To date, there is no evidence of intimate interactions between the two *b* subunits within the tether domain between positions K23 and D53.

F_1F_o complexes containing chimeric *b′* subunits were much less stable in vitro than complexes with chimeric *b* subunits. Within the E39-to-I86 segment there are 14 amino acids in the *E. coli* and *T. elongatus b* subunits that are different in subunit *b′* (Fig. 1). While it is possible that these specific amino acids have an important influence on F_1F_o complex stability, it seems more likely that the overall structure of the *b′* subunit does not necessarily favor maintenance of the intersubunit contacts needed for a stable enzyme in aqueous buffers. This view is supported by the observation that the levels of $b'_{E39\text{-}D53}$, $b'_{L54\text{-}I86}$, and $b'_{E39\text{-}I86}$ were all increased by coexpression with the cognate *b* subunit (Fig. 2). Therefore, the formation of chimeric *b*/*b′* heterodimeric F_1F_o complexes seems to stabilize the chimeric *b′* subunits in vitro.

ACKNOWLEDGMENTS

This work was supported by Public Health Service grant GM70978. We thank Mac O'Neil Plancher for participation in the study.

REFERENCES

1. **Bhatt, D., S. P. Cole, T. B. Grabar, S. B. Claggett, and B. D. Cain.** 2005. Manipulating the length of the *b* subunit F_1 binding domain in F_1F_o ATP synthase from *Escherichia coli*. J. Bioenerg. Biomembr. **37:**67–74.
2. **Cain, B.** 2000. Mutagenic analysis of the F_o stator subunits. J. Bioenerg. Biomembr. **32:**365–371.
3. **Capaldi, R. A., and R. Aggeler.** 2002. Mechanism of the F_1F_o-type ATP synthase, a biological rotary motor. Trends Biochem. Sci. **27:**154–160.
4. **Caviston, T. L., C. J. Ketchum, P. L. Sorgen, R. K. Nakamoto, and B. D. Cain.** 1998. Identification of an uncoupling mutation affecting the *b* subunit of F_1F_o ATP synthase in *Escherichia coli*. FEBS Lett. **429:**201–206.
5. **Del Rizzo, P. A., Y. Bi, and S. D. Dunn.** 2006. ATP synthase *b* subunit dimerization domain: a right-handed coiled coil with offset helices. J. Mol. Biol. **364:**735–746.
6. **Del Rizzo, P. A., Y. Bi, S. D. Dunn, and B. H. Shilton.** 2002. The "second stalk" of *Escherichia coli* ATP synthase: structure of the isolated dimerization domain. Biochemistry **41:**6875–6884.
7. **Dickson, V. K., J. A. Silvester, I. M. Fearnley, A. G. W. Leslie, and J. E. Walker.** 2006. On the structure of the stator of the mitochondrial ATP synthase. EMBO J. **25:**2911–2918.
8. **Dunn, S. D., and J. Chandler.** 1998. Characterization of the $b_{2\delta}$ complex from *Escherichia coli* ATP synthase. J. Biol. Chem. **273:**8646–8651.
9. **Dunn, S. D., D. T. McLachlin, and M. Revington.** 2000. The second stalk of *Escherichia coli* ATP synthase. Biochim. Biophys. Acta **1458:**356–363.
10. **Dunn, S. D., E. Kellner, and H. Lill.** 2001. Specific heterodimer formation by the cytoplasmic domains of the *b* and *b′* subunits of cyanobacterial ATP synthase. Biochemistry **40:**187–192.
11. **Dunn, S. D., R. G. Tozer, and V. D. Zadorozny.** 1990. Activation of *Escherichia coli* F_1-ATPase by lauryldimethylamine oxide and ethylene glycol: relationship of ATPase activity to the interaction of the ε and β subunit. Biochemistry **29:**4335–4340.
12. **Galkin, M. A., R. R. Ishmukhametov, and S. B. Vik.** 2006. A functionally inactive, cold-stabilized form of the *Escherichia coli* F_1F_o ATP synthase. Biochim. Biophys. Acta **1757:**206–214.
13. **Gardner, J. L., and B. D. Cain.** 1999. Amino acid substitutions in the *a* subunit affect the ε subunit of F_1F_o ATP synthase from *Escherichia coli*. Arch. Biochem. Biophys. **361:**302–308.
14. **Grabar, T. B., and B. D. Cain.** 2004. Genetic complementation between mutant *b* subunits in F_1F_o ATP synthase. J. Biol. Chem. **279:**31205–31211.
15. **Grabar, T. B., and B. D. Cain.** 2003. Integration of *b* subunits of unequal length into F_1F_o-ATP synthase. J. Biol. Chem. **278:**34751–34756.
16. **Hardy, A. W., T. B. Grabar, D. Bhatt, and B. D. Cain.** 2003. Mutagenesis studies of the F_1F_o ATP synthase *b* subunit membrane domain. J. Bioenerg. Biomembr. **35:**389–397.
17. **McCormick, K. A., and B. D. Cain.** 1991. Targeted mutagenesis of the *b* subunit of F_1F_o ATP synthase in *Escherichia coli*: Glu-77 through Gln-85. J. Bacteriol. **173:**7240–7248.
18. **McLachlin, D. T., A. M. Coveny, S. M. Clark, and S. D. Dunn.** 2000. Site-directed cross-linking of the *b* to the α, β, and *a* subunits of the *Escherichia coli* ATP synthase. J. Biol. Chem. **275:**17571–17577.
19. **McLachlin, D. T., J. A. Bestard, and S. D. Dunn.** 1998. The *b* and δ subunit of the *Escherichia coli* ATP synthase interact via residues in their C-terminal regions. J. Biol. Chem. **273:**15162–15168.
20. **Motz, C., T. Hornung, M. Kersten, D. T. McLachlin, S. D. Dunn, J. G. Wise, and P. D. Vogel.** 2004. The subunit *b* dimer of the F_oF_1-ATP synthase: interaction with F_1-ATPase as deduced by site-specific spin-labeling. J. Biol. Chem. **279:**49074–49081.

21. **Nakamura, Y., T. Kaneko, S. Sato, M. Ikeuchi, H. Katoh, S. Sasamoto, A. Watanabe, M. Iriguchi, K. Kawashima, T. Kimura, Y. Kishida, C. Kiyokawa, M. Kohara, M. Matsumoto, A. Matsuno, N. Nakazaki, S. Shimpo, M. Sugimoto, C. Takeuchi, M. Yamada, and S. Tabata.** 2002. Complete genome structure of the thermophilic cyanobacterium *Thermosynechococcus elongatus* BP-1. DNA Res. **9:**123–130.
22. **Noji, H., and M. Yoshida.** 2001. The rotary machine in the cell, ATP synthase. J. Biol. Chem. **276:**1665–1668.
23. **Okajima, K., S. Yoshihara, Y. Fukushima, X. Geng, M. Katayama, S. Higashi, M. Watanabe, S. Sato, S. Tabata, Y. Shibata, S. Itoh, and M. Ikeuchi.** 2005. Biochemical and functional characterization of BLUF-type flavin-binding proteins of two species of cyanobacteria. J. Biochem. **137:** 741–750.
24. **Pattanayek, R., D. R. Williams, S. Pattanayek, Y. Xu, T. Mori, C. H. Johnson, P. L. Stewart, and M. Egli.** 2006. Analysis of KaiA-KaiC protein interactions in the cyanobacterial circadian clock using hybrid structural methods. EMBO J. **25:**2017–2028.
25. **Peng, G., M. Bostina, M. Radermacher, I. Rais, M. Karas, and H. Michel.** 2006. Biochemical and electron microscopic characterization of the F_1F_o ATP synthase from the hyperthermophilic eubacterium *Aquifex aeolicus*. FEBS Lett. **580:**5934–5940.
26. **Revington, M., D. T. McLachlin, G. S. Shaw, and S. D. Dunn.** 1999. The dimerization domain of the *b* subunit of the *Escherichia coli* F_1F_o-ATPase. J. Biol. Chem. **274:**31094–31101.
27. **Richter, M. L., R. Hein, and B. Huchzermeyer.** 2000. Important subunit interactions in the chloroplast ATP synthase. Biochim. Biophys. Acta **1458:** 326–342.
28. **Rodgers, A. J. W., and R. A. Capaldi.** 1998. The second stalk composed of the *b*- and δ-subunits connects F_o to F_1 via an α-subunit in the *Escherichia coli* ATP synthase. J. Biol. Chem. **273:**29406–29410.
29. **Rodgers, A. J. W., S. Wilkens, R. Aggeler, M. B. Morris, S. M. Howitt, and R. A. Capaldi.** 1997. The subunit δ-subunit *b* domain of *Escherichia coli* F_1F_o ATPase. J. Biol. Chem. **272:**31058–31064.
30. **Senior, A. E., S. Nadanaciva, and J. Weber.** 2002. The molecular mechanism of ATP synthesis by F_1F_o-ATP synthase. Biochim. Biophys. Acta **1553:**188–211.
31. **Smith, P. K., R. I. Krohn, G. T. Hermanson, A. K. Mallia, F. H. Gartner, M. D. Provenzano, E. K. Fujimoto, N. M. Goeke, B. J. Olson, and D. C. Klenk.** 1985. Measurement of protein using bicinchoninic acid. Anal. Biochem. **150:**76–85.
32. **Sorgen, P. L., M. R. Bubb, and B. D. Cain.** 1999. Lengthening the second stalk of F_1F_o ATP synthase in *Escherichia coli*. J. Biol. Chem. **274:**36261–36266.
33. **Sorgen, P. L., M. R. Bubb, K. A. McCormick, A. S. Edison, and B. D. Cain.** 1998. Formation of the *b* subunit dimer is necessary for interaction with F_1-ATPase. Biochemistry **37:**923–932.
34. **Sorgen, P. L., T. L. Caviston, R. C. Perry, and B. D. Cain.** 1998. Deletions in the second stalk of F_1F_o-ATP synthase in *Escherichia coli*. J. Biol. Chem. **273:**27873–27878.
35. **Weber, J.** 2006. ATP synthase: subunit-subunit interactions in the stator stalk. Biochim. Biophys. Acta **1757:**1162–1170.